Excited state spectroscopy by ionic projection

ter Steege, D.H.A.

Publication date
2003

CHAPTER THREE

VIBRONIC COUPLING IN EXCITED STATES OF ACETONE [♦]

ABSTRACT

Photoelectron spectroscopy of Rydberg states of acetone-h_6 and $-d_6$ populated by two- or three-photon excitation has been employed to unravel the vibronic description of excited-state levels. For the 3p Rydberg states vibronic transitions have been reanalysed, leading to various reassignments and the observation of hitherto non-reported transitions. In addition, several ionic vibrational frequencies could be determined. At higher excitation energies previously identified, and in the present study newly identified, members of two Rydberg series have been characterised. The ns Rydberg series was explored up to the 8s state, the nd series up to the 7d state. Based upon the unambiguous assignments of vibronic character that we obtain for excited-state levels, various valence-Rydberg and Rydberg-Rydberg vibronic coupling pathways come to light and are analysed.

[♦] D.H.A. ter Steege, A.C. Wirtz, and W.J. Buma, J. Chem. Phys. **116**, 1 (2002).

3.1 INTRODUCTION.

Acetone is the simplest aliphatic derivative of the carbonyl family. As such, it is an obvious choice for studying the spectroscopic and dynamic properties of the excited states of this family of homologues. The photoresponse of carbonyl containing compounds, for example in the form of photodissociation of ketones, is important in photobiology for various reasons, amongst which the fact that three out of four DNA bases contain such functional groups. Because of its simplicity, small size, and central position in many areas of chemistry, the interpretation of the electronic spectrum of acetone has been, and still is subject of many spectroscopic studies. Theoretical studies of the spectroscopic properties of carbonyl compounds have, however, mainly been focussed on formaldehyde (H_2CO) [1-3]. A few *ab initio* studies on the excited states of acetone have been performed at various levels of sophistication [4-8]. These calculations considered mainly the $n\pi^*$, $\pi\pi^*$, and $\sigma\pi^*$ valence states, as well as the lower-lying n=3 and n=4 Rydberg states

Acetone belongs to the C_{2v} symmetry point group, with the z-axis along the C=O bond and the CCOC skeleton in the yz plane and the electronic configuration $\ldots(2b_1)^2(5b_2)^2(3b_1)^0$ in its 1^1A_1 ground state. Vibrational frequencies of the ground state have been compiled by Shimanouchi [9] and are given in Tables I and II for acetone-h_6 and -d_6, respectively. For the comparison with other studies, particularly those of Goodman *et al.* [10] and McDiarmid *et al.* [11], it is important to notice that two notations seem to be in use. This alternative numbering of vibrations is indicated in the Tables as well. The $\nu_{12}(a_2)$ anti-gearing and $\nu_{24}(b_1)$ (alternatively labelled as ν_{17}) gearing modes have attracted particular attention in the context of understanding torsional potential interactions in coupled methyl tops in the electronic ground, excited, and ionic states of acetone [10,12-15].

The highest occupied molecular orbital ($5b_2$) is a non-bonding orbital, which in first approximation can be represented by the $2p_y$ atomic orbital on oxygen [7]. Concentrating on the singlet manifold, we see that excitation from this lone pair orbital n_y to the $3b_1(\pi^*)$ orbital leads to the first excited singlet valence state 1^1A_2 that

has its 0-0 transition at 30439.9145 cm^{-1} [16]. This dipole-forbidden transition has been the subject of many experimental studies [17-20] concentrating on aspects such as the role of vibronic coupling and interaction with triplet states [16,21,22]. The first Rydberg state derives from excitation of a lone pair electron to the 3s Rydberg orbital, giving rise to the 1^1B_2 state located at 6.35 eV[14,23-26]. Vibronic coupling comes prominently forward in the excitation spectra of this state by the activity of the $\nu_{12}(a_2)$ and $\nu_{24}(b_1)$ nontotally-symmetric vibrations [14].

In the present study we will primarily be concerned with the 3p and higher Rydberg states. In particular the 3p Rydberg states have been the subject of extensive research, starting with various efforts to establish the order of the $3p_x$ (2^1A_2), $3p_y$ (2^1A_1), and $3p_z$ (2^1B_2) states [24,27]. The comparison of the one-photon absorption spectrum with the two-photon Resonance Enhanced MultiPhoton Ionisation (REMPI) spectrum under linearly and circularly polarised excitation light conditions ultimately enabled the unambiguous assignment of the origin transitions found at 7.36, 7.41, and 7.45 eV as deriving from the $3p_x$, $3p_y$, and $3p_z$ states, respectively [11,24,27,28]. Photoacoustic spectroscopy [28] demonstrated dramatic differences in the radiationless decay channels available to the three Rydberg states. In particular the $3p_y$ Rydberg state was considered to be subject to considerable mixing with the $\pi\pi^*$ ($^1A_1$) valence excited state [29], although for the $3p_z$ Rydberg state some mixing with an $n\sigma^*$ valence excited state was invoked as well [28]. Subsequent extensive studies of the two- and three-photon excitation spectra of the 3p Rydberg states and their polarization dependence led to assignments of active vibrations in the excitation spectrum [7,11,27]. In these excitation spectra anomalously intense vibrational bands at high vibrational energies could be observed that were attributed to the effects of vibronic coupling with the $\pi\pi^*$ state. Their presence led to an approximate location of the $\pi\pi^*$ state between 7.5 and 7.7 eV, approximately where the $\pi\pi^*$ and A_1 $3p_y$ Rydberg potential curves were calculated to cross. Despite many efforts, however, direct observation of this valence excited state has been unsuccessful.

Table 3.1: *Experimental and ab initio vibrational frequencies (cm^{-1}) of ground, excited, and ionic states of acetone-h_6* [a].

sym	ν	mode	alt.[b]	X^1A_1	$3p_x$ ($^1A_2$)	$3p_y$ ($^1A_1$)	$3p_z$ ($^1B_2$)	X^2B_2 [c]		B3LYP X^2B_2 [d]
a_1	1	CH_3-d-stretch		3019		3128	3148			3084
a_1	2	CH_3-s-stretch		2937		2424				2940
a_1	3	CO strectch		1731	1468 [e]			1541 [e]	(1548)	1570
a_1	4	CH_3-d-deform		1435	1395 [e]		1376 [e]	1410 [e]		1395
a_1	5	CH_3-s-deform		1364	1293	1309	1280 [e]		(1288)	1269
a_1	6	CH_3 rock		1066	1050 [e]	1058 [e]	1042 [e]	1046 [e]	(1049)	1045
a_1	7	CC stretch		777				682 [e]		675
a_1	8	CCC deform		385 [f]	326.2	324 [e]	316 [e]	339 [e]	(313)	321
a_2	9	CH_3-d-stretch		2963						3007
a_2	10	CH_3-d-deform		1426	1432 [e]			1484 [e]		1400
a_2	11	CH_3 rock		877	892 [e]					868
a_2	12	Torsion		77.8	70.8	70		66.7		-49
b_2	13	CH_3-d-stretch	18	3019						3083
b_2	14	CH_3-s-stretch	19	2937						2933
b_2	15	CH_3-d-deform	20	1410						1385
b_2	16	CH_3-s-deform	21	1364						1313
b_2	17	CC stretch	22	1216						984
b_2	18	CH_3-rock	23	891			868 [e]			882
b_2	19	CO ip-bend	24	530			366 [e]	359 [e]		350
b_1	20	CH_3-d-stretch	13	2972						3014
b_1	21	CH_3-d-deform	14	1454						1424
b_1	22	CH_3-rock	15	1091						1032
b_1	23	CO op-bend	16	484 [f]	453	484				454
b_1	24	Torsion	17	124.5	129.4					116

[a] experimental frequencies taken from Refs. [9,11,13,15,25], except those labeled [e].
[b] alternative numbering employed for example in Refs. [11] and [13].
[c] frequencies reported in the He(I) photoelectron study of Ref. [41] are given in parentheses.
[d] after scaling with factor 0.9614 [48].
[e] frequency determined in present work.
[f] assignments of ν_8 and ν_{23} in the ground state have been subject of discussion [9,16,27,49].

Table 3.2: *Experimental and ab initio vibrational frequencies (cm^{-1}) of ground, excited, and ionic states of acetone-d_6*[a].

sym	v	mode	alt[b]	X^1A_1	$3p_x$ ($^1A_2$)	$3p_y$ ($^1A_1$)	$3p_z$ ($^1B_2$)	X^2B_2	B3LYP X^2B_2[c]
a_1	1	CH_3-d-stretch		2264	2433		2411		2291
a_1	2	CH_3-s-stretch		2123	2165	1792			2108
a_1	3	CO strectch		1732					1534
a_1	4	CH_3-d-deform		1080	1028[d]		1022[d]	1030[d]	1023
a_1	5	CH_3-s-deform		1035	969[d]			966[d]	967
a_1	6	CH_3 rock		887	823[d]	832[d]	817[d]	798[d]	826
a_1	7	CC stretch		689	672	660	665	669[d]	633
a_1	8	CCC deform		320[e]	279.5	278[d]	275[d]	234[d]	277
a_2	9	CH_3-d-stretch		2205					2228
a_2	10	CH_3-d-deform		1021	1109[d]			1113[d]	1012
a_2	11	CH_3 rock		669	671[d]			678[d]	657
a_2	12	Torsion		53.4	49.1			42.4	-34
b_2	13	CH_3-d-stretch	18	2264					2287
b_2	14	CH_3-s-stretch	19	2123					2103
b_2	15	CH_3-d-deform	20	1004			877[d]		898
b_2	16	CH_3-s-deform	21	1035					988
b_2	17	CC stretch	22	1242					1033
b_2	18	CH_3-rock	23	724					704
b_2	19	CO ip-bend	24	475			345[d]	355[d]	332
b_1	20	CH_3-d-stretch	13	2227					2232
b_1	21	CH_3-d-deform	14	1050					1025
b_1	22	CH_3-rock	15	960					888
b_1	23	CO op-bend	16	405[e]					383
b_1	24	Torsion	17	96.0	98.2	100			87

[a] experimental frequencies taken from Refs. [9,11,13,15,25], except those labeled [d].
[b] alternative numbering employed for example in Refs. [11] and [13].
[c] after scaling with factor 0.9614 [48].
[d] frequency determined in present work.
[e] assignments of ν_8 and ν_{23} in the ground state have been subject of discussion [9,16,27,49].

Starting with the 3d Rydberg states, information on the higher excited states becomes scarcer. Partly on the basis of *ab initio* calculations, the $3d_{x^2-y^2}$ (3^1B_2) and $3d_{xy}$ (2^1B_1) Rydberg states were assigned to three-photon resonances found at 8.09 and 8.17 eV, while the $3d_{yz}$ (3^1A_1) state was associated with a diffuse broad absorption band around 7.8 eV [7]. This state was proposed to be perturbed by the $\pi\pi^*$ valence state in a similar way as the $3p_y$ Rydberg state. In the same multiphoton ionisation study, two of the three 4p Rydberg states were identified at 8.55 and 8.60 eV on the basis of their quantum defect. Evidence for Rydberg states higher than 4p has been reported in two early absorption studies [30,31]. At that time, however, no conclusive assignments were made.

In the present work we will apply excited-state photoelectron spectroscopy to study the spectroscopic and dynamic properties of the Rydberg manifold of acetone starting with the 3p Rydberg states. As amply demonstrated in previous studies [32-36], this approach has unique advantages over the commonly employed approach of mass-resolved ion detection, since in general it allows the unambiguous identification of the (ro)vibronic character of the excited state from which ionisation took place. Put in another way, one might say that the projection of the wavefunction of the excited state on the ionic manifold, as done in the photoionisation step, ultimately enables the reconstruction of this wavefunction. As will be shown, these characteristics enable us to elucidate various aspects of the electronic structure of acetone, in particular those related to vibronic coupling between excited states. Although previous studies have paved the way for the assignment of the rich vibrational structure observed in the excitation spectra of the 3p Rydberg states [7,11], the fact that these three states are energetically so close together has inhibited a definite assignment of all resonances. Indeed, it will become clear that various previous assignments need to be revised or refined. At higher excitation energies previously identified Rydberg states have been characterised, and new states identified up to the 8s Rydberg state. A common theme evident from all photoelectron spectra is that vibronic coupling pervades at all possible levels, be it between Rydberg and valence states, be it between the various

components of one Rydberg state, *e.g.*, $3p_x$. $3p_y$, and $3p_z$, or be it between Rydberg states with Rydberg electrons of different angular momentum or principal quantumnumber. In fact, it will be shown that in the present study some of the identified Rydberg states are "unobservable" in our excitation spectra, but become observable by vibronic coupling in the photoelectron spectra of other states. Finally, as a spin-off, the present study has enabled the determination of the, till now unknown, frequency of several vibrations in the ground state of the acetone radical cation.

3.2 EXPERIMENTAL AND THEORETICAL DETAILS.

The setups we use have been described in great detail previously [37,38] and will therefore only be summarized briefly here. In our experiments we partly made use of samples seeded into supersonic expansions, but also performed studies using effusive beams. The high-resolution (2+1) Resonantly Enhanced MultiPhoton Ionisation (REMPI) spectra and PhotoElectron spectra (PES) of supersonically cooled acetone and deuteroacetone have been measured using a pulsed dye laser running on DCM dissolved in DMSO (Lumonics Hyperdye-300), which was pumped by a XeCl excimer laser (Lambda Physik EMG103MSC). This excimer laser gives 10 ns pulses with a maximum pulse energy of 200 mJ and is typically used at a repetition rate of 30 Hz. The dye laser output was frequency doubled using an angle-tuned KD*P crystal in an INRAD II autotracker and focused by a 25 mm quartz lens into the ionisation region of the spectrometer. This spectrometer consists of a 2π analyser that has been slightly modified from the original design by Kruit and Read [39], and has been interfaced with a pulsed molecular beam. In the ionisation region of the spectrometer a strongly diverging magnetic field parallelises the trajectories of the electrons produced in a laser shot. The kinetic energies of the electrons are subsequently analysed by means of a time-of-flight technique. After detection by a pair of microchannel plates, the signal is stored in a 500 MHz digital oscilloscope (Tektronix TDS540), which is connected to a computer (Intel 80486 DX2 66 MHz).

An excitation spectrum is constructed by integration of (part of) the photoelectrons over the scanned wavelength region. Photoelectron spectra are recorded by increasing in steps the retarding voltage on a grid surrounding the flight tube, and transforming each time only the high-resolution part of the time-of-flight spectrum. In this way, an optimum energy resolution of about 10 meV can be obtained for all kinetic energies. The energy scale of the photoelectrons as well as the laser wavelengths were calibrated using multiphoton resonances of krypton or xenon [40].

The pulsed supersonic expansion is generated by expansion of 3 bar He mixed with room-temperature acetone vapour through a 0.5 mm diameter pulsed nozzle (General Valve Iota One System) into a chamber that is pumped by an Edwards Diffstak 2000 oil diffusion pump backed by an Edwards E2M40 rotary pump. The expansion chamber is connected through a Beam Dynamics skimmer with a diameter of 0.5 mm to the ionisation chamber, which in turn is evacuated by a Balzers TPH 170 turbomolecular pump backed by a Leybold Trivac D16B rotary pump. The flight tube is pumped by a Leybold Turbovac 450 turbomolecular pump backed by a Leybold Trivac D16B rotary pump. A pulse duration of typically 200 μs at a repetition rate of 30 Hz resulted in a pressure in the expansion chamber of about 6×10^{-5} mbar. Without gas input the pressure is about 1×10^{-7} mbar. The pressure in the flight tube is typically 1×10^{-7} mbar, and remains basically the same under operating conditions. A home-built delay generator is used to control the timing of the gas pulse relative to the laser pulse.

(3+1) REMPI experiments have been performed on effusively introduced samples using a laser system that consists of a pulsed dye laser (Lumonics Hyperdye-500, bandwidth ~0.08 cm^{-1}) pumped by a Lumonics HyperEx-460 excimer laser. For the (3+1) experiments several dyes have been used: Coumarine 480, 460, and 440 and Exalite 428, 416, 411, 404, 398 and 389. The laser beam is in these effusive experiments focussed into the ionisation region of a first-generation magnetic bottle

electron spectrometer by a 25 mm quartz lens. Commercially available acetone-h_6 and $-d_6$ were used as supplied.

In conventional electron-detected excitation spectroscopy all photoelectrons, irrespective of their kinetic energies, are collected and their yield monitored during the scan. In the present study we will be interested in monitoring electrons that derive from ionisation to very well-defined ionic levels. In order to accomplish this with a good energy resolution, we have to retard the electrons in the flight tube, but at the same time take care that during a scan over a rather large energy range these electrons still arrive within a preset gate. This has been realised by employing a wavelength dependent retarding voltage on the flight tube.

For the analysis of our high-resolution photoelectron spectra it turned out to be necessary to have a rather accurate idea of ionic vibrational frequencies. In the past a few of these frequencies have been determined [10,15,41], but not enough to serve our purpose. Following previously reported calculations [10], we have therefore performed *ab initio* calculations of the equilibrium geometry and the associated harmonic force field at the UB3LYP/6-31G* [42-44] level employing the Gaussian suite of programs [45]. These calculations have been done assuming C_{2v} symmetry of the molecule with an eclipsed-eclipsed geometry of the methyl groups, and lead to the frequencies reported in Tables I and II for acetone-h_6 and $-d_6$, respectively. From these Tables it can be seen that for ν_{12} an imaginary frequency is calculated. We do not interpret this as an indication for a departure from C_{2v} symmetry in the $X\ ^2B_1$ ionic ground state, rather that at this level the employed method is not adapted to deal with the flat potential energy surface along ν_{12}. Indeed, other studies [10] report that the eclipsed-eclipsed geometry of the molecule is a stable minimum on the potential energy surface of the radical cation.

3.3 RESULTS AND DISCUSSION.

3.3.1. (2+1) REMPI-PES of supersonically cooled acetone-h_6 and $-d_6$.

In Figure 1 the two-photon resonance enhanced multiphoton ionisation spectra of supersonically cooled acetone-h_6 and acetone-d_6 in the two-photon energy range of 59200 to 62200 cm^{-1} are shown. In this excitation region the 3p Rydberg states have been located previously [10-13,15,24,27-29]. The excitation spectra show various resonances that are tabulated in Tables III and IV for acetone-h_6 and -d_6, respectively. Their assignments have been done on the basis of photoelectron spectra recorded at these resonances, utilizing the calculated ionic frequencies referred to in the previous section. The vibrational frequencies that have been determined for the various states on the basis of these assignments are collected in Tables I and II for acetone-h_6 and -d_6, respectively. Although this particular part of the excitation region has been extensively investigated in the past [11], it will become clear that the application of excited-state photoelectron spectroscopy leads to new insights in the spectroscopic and dynamic properties of the excited states. To this purpose we will show and discuss in the following some typical photoelectron spectra.

The (2+1) photoelectron spectrum of acetone-h_6 taken at the 0-0 transition to the $3p_x$ ($^1A_2$) state (59360 cm^{-1}) [11] is depicted in Figure 2a. The spectrum shows only one peak with an energy of 1.333±0.005 eV, which - employing a lowest ionisation energy of 9.708 eV [15] - can be assigned as deriving from an ionisation process, starting from a vibrationless ground state, $\mathbf{v}''=0$, to the vibrationless ionic state, $\mathbf{v}^+=0$. We will abbreviate such a $\mathbf{v}^+=0 \leftarrow \mathbf{v}''=0$ ionisation as the $0''\text{-}0^+$ peak in the rest of this paper. The corresponding photoelectron spectrum for acetone-d_6 (not shown) was taken at 59363 cm^{-1} and displays, apart from the dominant peak associated with ionisation to the $\mathbf{v}^+=0$, a small peak shifted by 121 meV (976 cm^{-1}) from the $0''\text{-}0^+$ peak, which can be assigned to ionisation to the $\nu_5^+=1$ level on the basis of the calculated ionic frequencies. The observation of a predominant $\Delta\mathbf{v}=\mathbf{v}^+\text{-}\mathbf{v}''=0$ behaviour strongly suggests that the equilibrium geometry and potential energy surface of the $3p_x$ Rydberg state and of the ground ionic state are very similar, in agreement with the conclusions drawn from previous ZEKE-PFI studies [10,15].

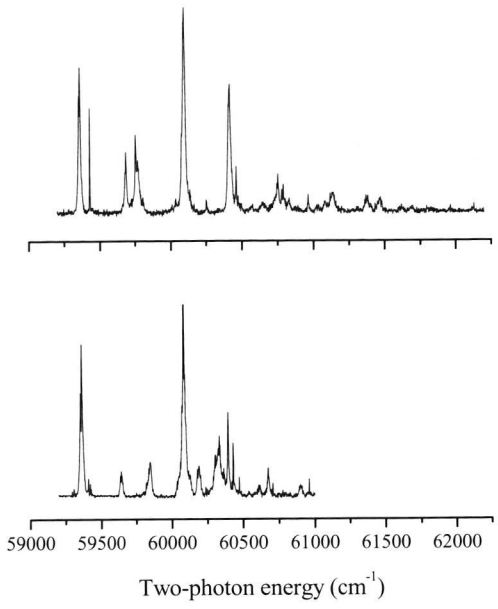

Figure 3.1: *(2+1) REMPI spectrum of jet-cooled acetone-h_6 (top) and acetone-d_6 (bottom).*

The photoelectron spectrum depicted in Figure 2b was recorded at a two-photon energy of 59684 cm^{-1}. This resonance was previously assigned to the $(3p_x)8_0^1$ transition [11]. In that case $\Delta v=0$ behaviour would lead us to expect that ionisation *via* this resonance should predominantly lead to ions in the $\nu_8^+=1$ level. The spectrum shows a small peak at 1.396±0.005 eV deriving from ionisation to the vibrationless ion, and an intense peak peak shifted 41 meV from the 0"-0^+ peak, which indeed arises from ionisation to the $\nu_8^+=1$ level. This spectrum thus not only confirms the previous assignment [11], but also gives insight in the vibrational frequencies in the ionic ground state of acetone. From this spectrum and others, we can conclude that the ν_8 ionic vibrational frequency is 42±3 meV (339±24 cm^{-1}). The $(3p_x)8_0^1$ transition in acetone-d_6 is found at 59642 cm^{-1}. Ionisation *via* this state leads to a photoelectron

spectrum similar to the one obtained for acetone-h_6: an intense $\Delta v=0$ peak is seen that is shifted by 29±5 meV (234±40 cm^{-1}) from a non-observable $0''$-0^+ peak.

Table 3.3: *Observed two- and three-photon transitions for acetone-h_6 and their assignments. Assignments given in bold concern transitions that either have been reassigned or were not reported in previous studies.*

Two-photon	Three-photon	$3p_x(^1A_2)$		$3p_y(^1A_1)$		$3p_z(^1B_2)$	
$\bar{\nu}$ (cm^{-1})	$\bar{\nu}$ (cm^{-1})	$\Delta\bar{\nu}$ [a] (cm^{-1})	assignment	$\Delta\bar{\nu}$ [a] (cm^{-1})	assignment	$\Delta\bar{\nu}$ [a] (cm^{-1})	assignment
59360	59373	0	0_0^0				
59430		70	12_0^1				
59684		324	8_0^1				
59756		396	$8_0^1 12_0^1$				
59770	59797			0	0_0^0		
59810		450	$\mathbf{23_0^1 / 8_0^1 24_0^1}$				
60094	60110			324	8_0^1	0	0_0^0
60252		892	$\mathbf{11_0^1}$				
60410	60440	1050	6_0^1	640	8_0^2	316	8_0^1
60460						366	$\mathbf{19_0^1}$
60476		1116	$\mathbf{6_0^1 12_0^1}$				
60755		1395	$\mathbf{4_0^1}$				
60780						686	$\mathbf{8_0^1 19_0^1}$
60792	60786	1432	$\mathbf{10_0^1}$				
60828		1468	$\mathbf{3_0^1}$				
60962						868	$\mathbf{18_0^1}$
61136	61107					1042	6_0^1
61374						1280	5_0^1
61470	61470					1376	4_0^1
	62241			2471	2_0^1		
	62559			2789	$2_0^1 8_0^1$		

[a] $\Delta\bar{\nu}$ given relative to the two-photon origin transitions.

Figure 3.2: *(2+1) Photoelectron spectra of acetone-h_6 at (a) 59360 cm^{-1} ($(3p_x)\,0_0^0$); (b) 59684 cm^{-1} ($(3p_x)\,8_0^1$); (c) 59770 cm^{-1} ($(3p_y)\,0_0^0$); (e) 60094 cm^{-1} ($(3p_z)\,0_0^0$ and $(3p_y)\,8_0^1$); (f) 60460 cm^{-1} ($(3p_z)\,19_0^1$); (g) 60792 cm^{-1} ($(3p_x)\,10_0^1$); (h) 60828 cm^{-1} ($(3p_x)\,3_0^1$) and of acetone-d_6 at (d) 59846 cm^{-1} ($(3p_y)\,0_0^0$).*

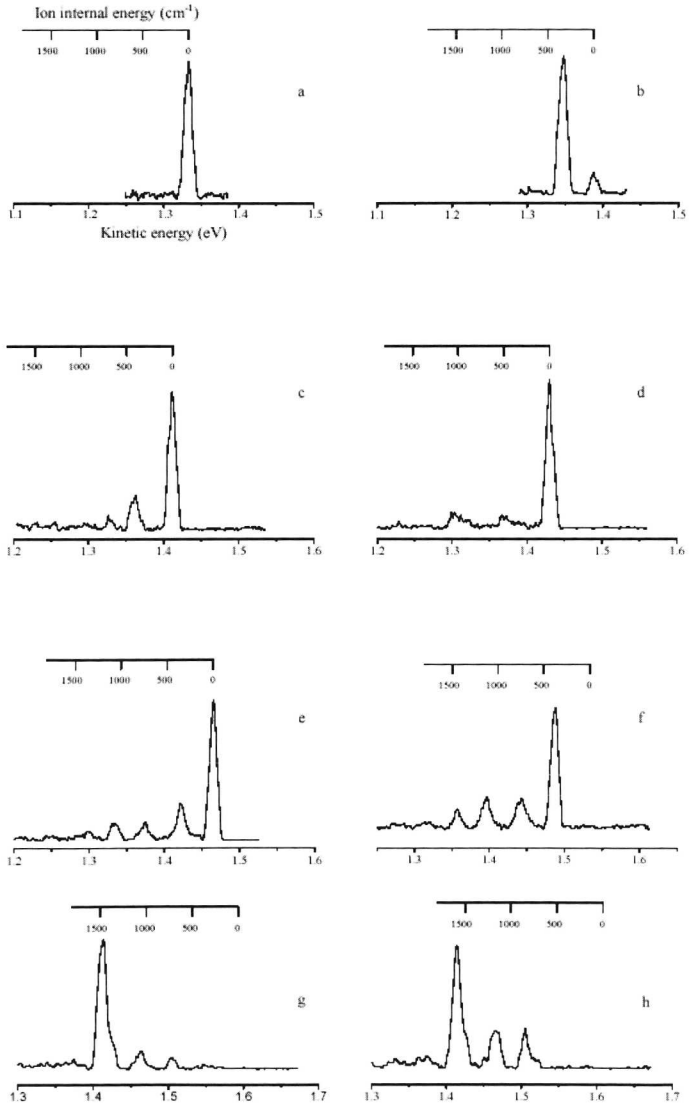

Table 3.4: *Observed two- and three-photon transitions for acetone-d_6 and their assignments. Assignments given in bold concern transitions that either have been reassigned or were not reported in previous studies.*

Two-photon	Three-photon	$3p_x(^1A_2)$		$3p_y(^1A_1)$		$3p_z(^1B_2)$	
$\bar{\nu}$ (cm^{-1})	$\bar{\nu}$ (cm^{-1})	$\Delta\bar{\nu}$ [a] (cm^{-1})	assignment	$\Delta\bar{\nu}$ [a] (cm^{-1})	assignment	$\Delta\bar{\nu}$ [a] (cm^{-1})	assignment
59363	59377	0	0_0^0				
59408		45	12_0^1				
59642		279	8_0^1				
59846	59835			0	0_0^0		
60034		671	$\mathbf{11_0^1}$				
60083	60094					0	0_0^0
60124				278	8_0^1		
60186		823	6_0^1				
60332		969	$\mathbf{5_0^1}$				
60358	60369					275	8_0^1
60391		1028	$\mathbf{4_0^1}$	545	8_0^2		
60428						345	$\mathbf{19_0^1}$
60472		1109	$\mathbf{10_0^1}$				
60678				832	6_0^1		
60706						626	$\mathbf{8_0^1 19_0^1}$
60900						817	6_0^1
60960						877	$\mathbf{15_0^1}$
	61105					1022	$\mathbf{4_0^1}$
	61327	1964	$\mathbf{5_0^2}$				
	61597			1751	2_0^1		

[a] $\Delta\bar{\nu}$ given relative to the two-photon origins.

As yet, the photoelectron spectra exhibit rather expected behaviour. This situation becomes quite different when ionisation *via* the 0-0 transition to the $3p_y(^1A_1)$ Rydberg state is considered. Normally, we would expect an intense 0"-0^+ peak, and although the photoelectron spectrum shown in Figure 2c does indeed show a 0"-0^+

peak at 1.409±0.005 eV, also two other peaks are seen. Under the supersonic conditions of our experiments our initial state is the vibrationless ground state. Within the Born-Oppenheimer approximation [46] only excitation of totally-symmetric vibrational levels would be permitted, and ionisation should thus in the end lead to ions that are also in totally-symmetric vibrational levels. The small peak displaced by 83 meV (669 cm^{-1}) from the 0"-0^+ peak can indeed be assigned without problem to ionisation to the $\nu_7^+(a_1)=1$ level (see Table I). However, the same Table shows that an assignment of the peak shifted by 50 meV (~ 400 cm^{-1}) in terms of a totally-symmetric vibrational level is not possible. We must therefore find another explanation for this peak. If we forget for the moment our symmetry considerations, we see that the ionic $8^1 12^1$ vibrational level of a_2 symmetry would have the correct vibrational energy. Ionisation to this level implies, however, excitation of the same vibrational level in the intermediate state. Now all pieces fall together because the only electronic state that would come into consideration to have this particular vibrational level close to the $3p_y$ state is the $3p_x(^1A_2)$ state. The *vibronic* symmetry of the $(3p_x)8^1 12^1$ level would then be A_1, *i.e.*, the same symmetry as the $3p_y$ Rydberg state. We thus have to come to the conclusion that the $(3p_x)8^1 12^1$ and $(3p_y)0^0$ levels are coupled on account of their near-degeneracy. As a result, the ionisation process does not only reveal the $(3p_y)0^0$ character, but also the coupled $(3p_x)8^1 12^1$ character.

Excitation of the $(3p_y)0^0$ level in acetone-d_6 has been reported to occur at a significantly higher energy [27]. Ionisation *via* this state was recorded at 59846 cm^{-1} and is shown in Figure 2d. We observe an intense peak at the 0"-0^+ position at 1.430 eV. A small broad peak is observed shifted by 56 meV (452 cm^{-1}). Inspection of Table II leads once again to the conclusion that this energy cannot be assigned to a totally-symmetric ionic vibrational level. On the other hand, the value of 56 meV matches very well the energy difference between the origin transitions to the $3p_x$ and $3p_y$ states. If we therefore assume that the peak finds its origin in the coupling between a $3p_x$ vibrational level with a_2 symmetry and the $3p_y$ vibrationless level, we find that it corresponds either to ionisation to the $8^1 12^3$ level (54 meV) or the $19^1 24^1$ level (52

meV). Notice that in the present case ionisation to the $8^1 12^1$ level can definitely be ruled out - in that case a peak at 40 meV would have been expected. From the intensity of the various peaks in Figure 2d it is clear that in acetone-d_6 the coupling of the $3p_y$ and the $3p_x$ states is less than in acetone-h_6, in line with the observation that the energy gap between the two coupled levels is smaller in acetone-h_6. The third peak, 122 meV (984 cm^{-1}) displaced from the $0''$-0^+ peak, is assigned to ionisation to the 5^1 ionic level, as we observed previously for ionisation *via* the vibrationless transition to the $3p_x$ state of acetone-d_6.

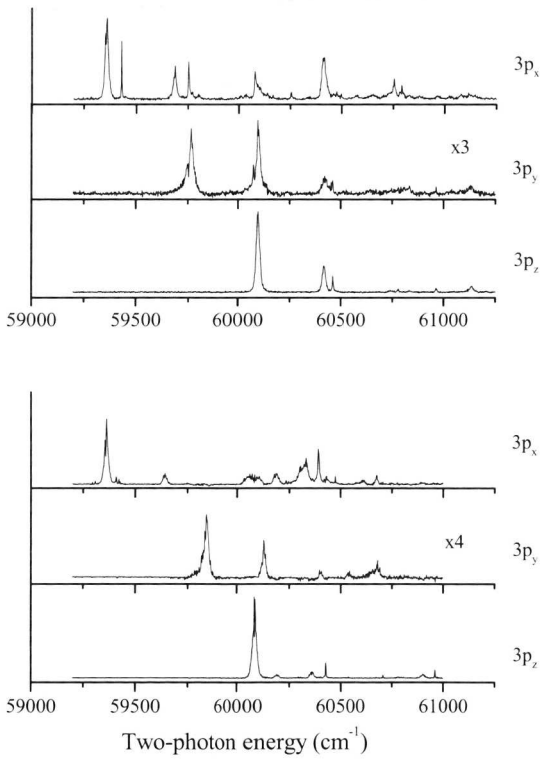

***Figure 3.3**: (2+1) REMPI spectra of jet-cooled acetone-h_6 (top) and acetone-d_6 (bottom) separated into the contributions of $3p_x$, $3p_y$, and $3p_z$ Rydberg states.*

In the last example a situation was encountered where we cannot unambiguously assign the ionic vibrational level to which ionisation occurs, simply because there are various possibilities that cannot be discriminated with our experimental resolution. At the same time we know that the ionic vibrational energy matches well the energy difference between two excited states, which implies that we do know the *electronic* character of the coupled state. It is clear that the higher we will go in excitation energy, the more this will occur on account of the increase in vibrational level density.

The photoelectron spectrum recorded at the $3p_z(^1B_2)$ origin for acetone-h_6 is shown in Figure 2e. In line with our expectations an intense 0"-0^+ peak is seen. We furthermore observe peaks shifted 43 meV (347 cm^{-1}), 92 meV (742 cm^{-1}), 131 meV (1057 cm^{-1}), and 169 meV (1363 cm^{-1}) from the 0"-0^+ peak. Again we will try to assign these peaks to totally-symmetric vibrational levels. In this spirit, the peaks at 169 meV and 131 meV are readily assigned to $\nu_4^+=1$ and $\nu_6^+=1$, respectively. Since in acetone-h_6 the $(3p_y)8_0^1$ transition is almost degenerate with the $3p_z$ origin transition, one would most logically assign the peak at 43 meV to ionisation to the $\nu_8^+=1$ level. This is, however, not the complete story. Firstly, below we will show excitation spectra in which we can visualise the contributions of the individual Rydberg states to the various resonances (Figure 3). The $3p_y$ trace shows there that the presumed $(3p_y)8_0^1$ transition has the same intensity as the $(3p_y)0_0^0$ transition. For the other two Rydberg states the 8_0^1 transition is significantly less intense than the 0_0^0 transition. Such a difference would *a priori* not be expected. Secondly, for acetone-d_6 the origin transition to the $3p_z$ state is not degenerate with the $(3p_y)8_0^1$ transition. The photoelectron spectrum obtained at the $(3p_z)0_0^0$ transition in acetone-d_6 shows, apart from an intense 0"-0^+ peak, a peak at 40 meV (323 cm^{-1}) that cannot be assigned to a totally-symmetric level, but matches very well the ionic frequency of the CO in-plane-bend ν_{19} of b_2 symmetry. This vibration is predicted to have an ionic frequency of 350 cm^{-1} in acetone-h_6 (Table I), and it may thus well be that the 43 meV peak in the

photoelectron spectrum of acetone-h_6 contains a contribution of ionisation to the ionic 19^1 level as well, thereby giving an explanation for the intensity anomaly noticed above. From the activity of ν_{19} in the photoelectron spectra we can conclude that vibronic coupling occurs between the $3p_z$ ($^1B_2$) and $3p_y$ ($^1A_1$) states.

For the 92 meV (742 cm^{-1}) peak in Figure 2e no appropriate a_1 vibrational level can be found. We notice that this energy is close to the energy difference between the $3p_x$ and $3p_z$ Rydberg states. It is therefore reasonable to assume that this peak results from the coupling of a $3p_x$ vibrational level with the $3p_z$ Rydberg state. Various possibilities such as the $8^1 23^1$ (96 meV), $7^1 24^1$ (98 meV), or even the $8^1 12^1 19^1$ (93 meV) come to mind. The observation of a peak at 89 meV (718 cm^{-1}) in the corresponding photoelectron spectrum of acetone-d_6 would slightly favour the $7^1 24^1$ assignment, but in the end there are simply too many possibilities that cannot be distinguished unambiguously with our experimental resolution. On top of that, it should be realised that because of different energy gaps, nontotally symmetric vibrational levels that are prominently visible for acetone-h_6 may not be visible for acetone-d_6 and vice versa. What can be said with reasonable certainty is, however, that the 92 meV (89 meV for -d_6) peak finds its origin in the ionisation of a vibrational level of the $3p_x$ Rydberg state.

The above examples, and many others not discussed here, clearly show that the dominant peaks in the photoelectron spectra derive from $\Delta v=0$ ionisation processes, be it from accessible vibrational levels of a certain Rydberg state, be it from levels that have become accessible by vibronic coupling. This implies that, when comparing ionisation *via* two different resonances associated with one particular Rydberg state, the kinetic energy of photoelectrons can be expected to have an absolute energy shift that is equal to the shift in photon energy. By setting gates in the time-of-flight spectrum on photoelectron peaks associated with $\Delta v=0$ ionisation from the $3p_x$, $3p_y$, and $3p_z$ Rydberg states, and compensating for changes in the electron kinetic energies when the excitation wavelength is scanned by adjusting the electric field in the flight tube – thus realising that these photoelectrons always arrive at the same time at the

detector – we are able to dissect the spectrum previously shown in Figure 1 into the contributions of the $3p_x$, $3p_y$, and $3p_z$ Rydberg states. The results for both acetone-h_6 and acetone-d_6 are shown in Figure 3. These spectra immediately show the previously discussed coupling between the three 3p states. An almost textbook example of the mixing of a bright and a dark state can be seen when the excitation spectrum of the 0-0 transition to the $3p_y$ state is considered (Figure 4). When electrons deriving from ionisation of $3p_x$ and $3p_y$ levels are monitored separately, a dip is observed in the $3p_y$ channel at 59756 cm^{-1}. This dip is exactly at the same place as the $8^1 12^1$ level of the $3p_x$ state. Mixing of the two levels results in a redistribution of intensity and we consequently see intensity appearing in the $3p_x$ channel at the same time that the intensity decreases in the $3p_y$ channel.

Another aspect of interest of the excitation spectra that is now elucidated are the rotational contours of the various resonances, which are seen to occur either as sharp or relatively broad. For identical photons - as is the case for the single laser experiments we are reporting here - the two-photon $T^2_{\pm 2,\pm 1,0}$ and the T^0_0 transition tensors may induce transition intensity [13, 47]. The former transition tensors give rise to $\Delta J=0$, ± 1, and ± 2 rotational transitions, the latter only to $\Delta J=0$ transitions. Simulations employing rotational constants of the ground state of the neutral and the radical cation confirm the suspicion that the sharp features should be interpreted as indicating a dominance of the T^0_0 tensor for these transitions. Because this tensor is totally-symmetric, we would in first instance expect the narrow resonances to be associated with transitions to the $3p_y(^1A_1)$ state. Such is not the case, as is clearly demonstrated in Figure 3: transitions to the $3p_y$ levels appear as "broad" features, while the "sharp" features are all associated with vibronically induced transitions to the $3p_x$ and $3p_z$ states. The observation that transitions to $3p_y$ levels appear as broad features while they would be expected to be narrow indicates that they are lifetime broadened. This would be in line with previous suspicions that the $3p_y$ state is subject to vibronic coupling with the valence excited $\pi\pi^*$ ($^1A_1$) state. Photoacoustic measurements [28, 29] give ample reason to believe that this $\pi\pi^*$ state has a very

short lifetime, and its mixing with the $3p_y$ state would thus lead to a shortening of the lifetime of this state - in agreement with our observations. Although our photoelectron spectra do not exhibit any direct signature of this $3p_y$ - $\pi\pi^*$ vibronic coupling, we can conclude that the excitation spectra indirectly give evidence for its presence.

From the traces shown in Figure 3, and the previously determined polarization behaviour of the resonances [11] we are now able to come to the unambiguous assignments given above in Tables III and IV. Our assignments differ in a number of cases with those of previous studies. In Tables III and IV these assignments are indicated in bold. In the following a number of the more prominent differences will be discussed.

The sharp line in the $3p_x$ channel spectrum at 60252 cm^{-1}, 892 cm^{-1} above the 0-0 transition, has been observed [11], but was not assigned. Its small width indicates that we deal here with a vibrational level of a_2 symmetry, and thus with a transition that obtains transition intensity by coupling with the $3p_y$ state. The most likely candidate is the CH_3 rock vibration ν_{11}. The corresponding $3p_x$ channel in acetone-d_6 shows a small sharp line 671 cm^{-1} shifted from the 0-0 transition. Upon deuteration the frequency of ν_{11} is observed to decrease from 877 to 669 cm^{-1} in the neutral ground state [9], and predicted to decrease from 868 cm^{-1} to 657 cm^{-1} in the ionic state. We can consequently safely assign the resonance to $(3p_x)11_0^1$ transition.

The resonance at 60460 cm^{-1} in the excitation spectrum of acetone-h_6 was previously assigned to the $(3p_y)23_0^2$ transition [11]. Figure 3 shows that at this excitation energy activity is observed in both the $3p_y$ and the $3p_z$ channels. Because of (i) its position - 366 cm^{-1} to the blue of the $3p_z$ origin - and (ii) its small width, we conclude that we deal here with the $(3p_z)19_0^1$ transition. Confirmation is found in the corresponding photoelectron spectrum (Figure 2f) that does not show a 0^+-0^+ transition, but a peak shifted by 46 meV from the theoretical 0^+-0^+ peak. The spectrum in Figure 2f shows a similar intensity pattern as seen in Figure 2e for ionisation via the 0-0 transition to the $3p_z$ state, all peaks being displaced, however, by the energy of the 19^1 ionic level. The peaks displaced by 92 meV and 139 meV can

now easily be assigned as deriving from ionisation from levels associated with the $3p_y$ and $3p_x$ states, while the peaks shifted by 219 meV and 179 meV from the 0"-0^+ peak correspond to ionisation to the $4^1 19^1$ and $6^1 19^1$ ionic levels, respectively. No evidence is found for a $(3p_y)23_0^2$ transition [11]. In acetone-d_6 we observe a similar transition at 60428 cm^{-1} that was previously assigned to the $(3p_y)23_0^2$ transition as well. On similar grounds as for acetone-h_6 we revise this assignment to the $(3p_z)19_0^1$ transition.

At 60755 cm^{-1} a broad line is observed for acetone-h_6 for which an photoelectron spectrum is obtained that shows only one intense peak shifted by 179 meV (1443 cm^{-1}) from the 0"-0^+ transition. This observation is at odds with the previous $(3p_y)8_0^3$ assignment, but would rather indicate ionisation to the $\nu_4^+=1$ level. Since the 60755 cm^{-1} resonance is shifted by 1395 cm^{-1} from the $(3p_x)0_0^0$ transition, we reassign it to the $(3p_x)4_0^1$ transition. The same transition is found for acetone-d_6 at 60395 cm^{-1}, 1032 cm^{-1} displaced from the $(3p_x)0_0^0$ transition. The associated photoelectron spectrum shows an intense peak 124 meV (1000 cm^{-1}) from the 0"-0^+ transition in agreement with the revised assignment.

The resonance observed at 60792 cm^{-1} in acetone-h_6 was previously thought to derive from the $(3p_y)6_0^1$ transition [11]. Its width and presence in the $3p_x$ channel indicates, however, that we deal here with a vibronic level of A_1 symmetry. Because the resonance is displaced by 1432 cm^{-1} from the $3p_x$ origin transition, we assign it as the $(3p_x)10_0^1$ transition. The photoelectron spectrum depicted in Figure 2g does not show a 0"-0^+ transition, but an intense peak at 184 meV (1484 cm^{-1}) that supports our assignment. Small peaks shifted by 134 meV (1081 cm^{-1}) and 95 meV (766 cm^{-1}) correspond to ionisation from levels associated with $3p_y$ and $3p_z$. In acetone-d_6 a similar resonance is observed in the $3p_x$ channel at 60472 cm^{-1}. This resonances was assigned as the $(3p_y)7_0^1$ transition [11], but since (i) the photoelectron spectrum reveals an intense peak 138 meV (1113 cm^{-1}) from the 0"-0^+ transition, (ii) it is 1110 cm^{-1} shifted from the $(3p_x)0_0^0$ transition, and (iii) its width does not support a

transition to a $3p_y$ vibrational level, we conclude that we deal here with the $(3p_x)10_0^1$ transition.

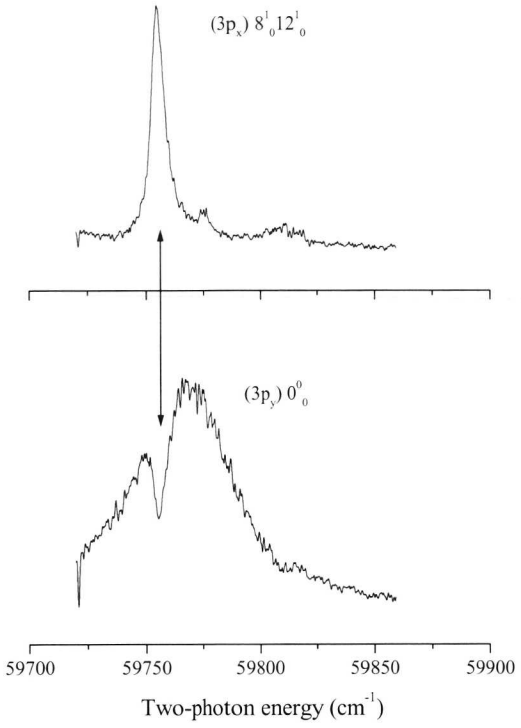

Figure 3.4: *Expanded view of the (2+1) REMPI spectrum of jet-cooled acetone-h_6 at the quasi-degenerate $(3p_x)12_0^18_0^1$ and $(3p_y)0_0^0$ transitions.*

We finally consider the resonance observed at 60828 cm^{-1} in the $3p_x$ channel of acetone-h_6, previously assigned to the $(3p_z)7_0^1$ transition. This resonance is shifted by 1468 cm^{-1} from the $(3p_x)0_0^0$ transition, and its photoelectron spectrum (Figure 2h) shows an intense peak shifted by 191 meV (1541 cm^{-1}) from the 0"-0^+ transition. Previous photoelectron spectra [41] and our *ab initio* calculations (Table I) indicate that this peak corresponds with ionisation to the $\nu_3^+=1$ level, which, in turn, implies

that the resonance should be assigned to the $(3p_x)3_0^1$ transition. Peaks in the photoelectron spectrum shifted by 131 meV and 91 meV arise from ionisation from levels associated with the $3p_y$ and $3p_z$ states.

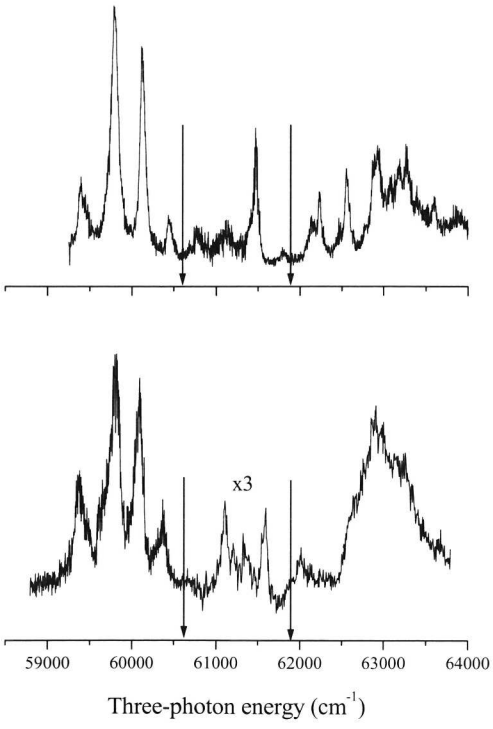

Figure 3.5: *(3+1) REMPI spectrum of room-temperature acetone-h_6 (top) and acetone-d_6 (bottom) in the region of 59000-64000 cm^{-1}. This spectrum is the composite of three different scans joint at the indicated excitation energies.*

The assignments as discussed above give evidence for various manifestations of vibronic coupling. In the case of the $3p_y$ state, interaction with the $\pi\pi^*$ valence state is not directly observed, but deduced, amongst else (*vide infra*), from the broadening of the two-photon resonances. Secondly, in the majority of the cases coupling occurs between a Franck-Condon allowed level and Franck-Condon forbidden levels on

account of near-degeneracy, as a result of which the Franck-Condon forbidden transition obtains intensity in the excitation step, while in the photoionisation step the multi-state description is dissected. Finally, Franck-Condon transitions are observed that do not become allowed by near-degeneracy of nontotally symmetric vibrational levels with allowed totally symmetric vibrational levels. These concern the transtions to a_2 vibrational levels of the $3p_x$ state, for example $(3p_x)12_0^1$, one transition to a b_1 vibrational level of this state, and transitions to b_2 vibrational levels of the $3p_z$ state. Although not seen in the present study, Kundu *et al.* [13] previously also observed the extremely weak $(3p_x)24_0^1$ transition, *i.e.*, a transition to a b_1 vibrational level of the $3p_x$ state. It has been suggested that for the $3p_x$ state a_2 modes might be particularly active because of the vibronic coupling that might occur then with the $\pi\pi^*$ valence state [14]. The present results, in combination with the two-photon transition probability coefficients calculated by Galasso [5], give a strong indication that the dominant coupling routes concern vibronic coupling *within* the 3p Rydberg manifold. The calculations predict that the two-photon excitation cross section of the $3p_x$ and $3p_z$ states are of the same order of magnitude, while the one of the $3p_y$ state is an order of magnitude larger. The two-photon excitation cross-section of the $\pi\pi^*$ state is in-between those of the $3p_{x,z}$ and $3p_y$ states. Indeed, it is found that all three origin transitions have an intensity that is of the same order of magnitude, bearing in mind, however, that the origin transition to the $3p_y$ state is severely lifetime broadened. On the basis of these calculated numbers one would thus predict (i) that because of the small energy differences, 3p interstate coupling is more effective than coupling with valence states, and (ii) that $3p_x \leftrightarrow 3p_y$ and $3p_z \leftrightarrow 3p_y$ coupling would be more effective in inducing two-photon transition intensity than $3p_x \leftrightarrow 3p_z$ coupling, in perfect agreement with our observations of $(3p_x)(a_2)_0^1$ and $(3p_z)(b_2)_0^1$ transitions, and the extreme weakness of a $(3p_x)(b_1)_0^1$ transition.

3.3.2. (3+1) REMPI-PES of acetone-h_6 and -d_6.

The spectral region above the 3p states has in the past not been investigated extensively. A few experimental results concerning excitation above the 3p states have been reported by Merchan *et al.* [7], who investigated acetone-h_6 and -d_6 by jet-cooled (3+1) REMPI in the energy region of 7.7-8.3 eV. Here they assigned transitions to 3d Rydberg states. As was noticed previously [11], (1+2) ionisation starts to interfere in this wavelength region, and we have therefore not pursued any additional two-photon excitation. In this section (3+1) REMPI results will be discussed that we have obtained in the energy region of 7.3-9.5 eV. The majority of these experiments have been performed under effusive conditions since previous experiments indicated that the widths of the three-photon resonances are significantly larger than the widths of the two-photon resonances, and that there is little to gain by performing jet-cooled experiments.

3.3.2.1. 58500 – 64200 cm^{-1} (7.2 – 7.9 eV) spectral region.

This area contains the 3p region that has been extensively investigated by (2+1) REMPI in previous studies [11,29] as well as in the previous section. The three-photon excitation spectra obtained with electron detection for acetone-h_6 under jet-cooled conditions and -d_6 under effusive conditions are shown in Figure 5, and agree with those reported in previous work using ion detection. Figure 5 shows that – when compared to the 0-0 transtions to the two other 3p states – the 0-0 transition to the $3p_y$ state is relatively more intense than in the (2+1) REMPI spectrum. The higher laser intensity required for (3+1) as compared to (2+1) multiphoton processes, advantages the ionisation process when it is in competition with decay processes from the excited state. The change in relative intensities may thus be taken as further evidence for the short-lived nature of the $3p_y$ Rydberg state. Photoelectron spectra have been measured for various resonances of both acetone-h_6 and -d_6 and were found to confirm the assignments and conclusions reported in the previous section. The spectral region containing the high-energy part of the 3p excitation region that has not been investigated using two-photon excitation needs some further discussion.

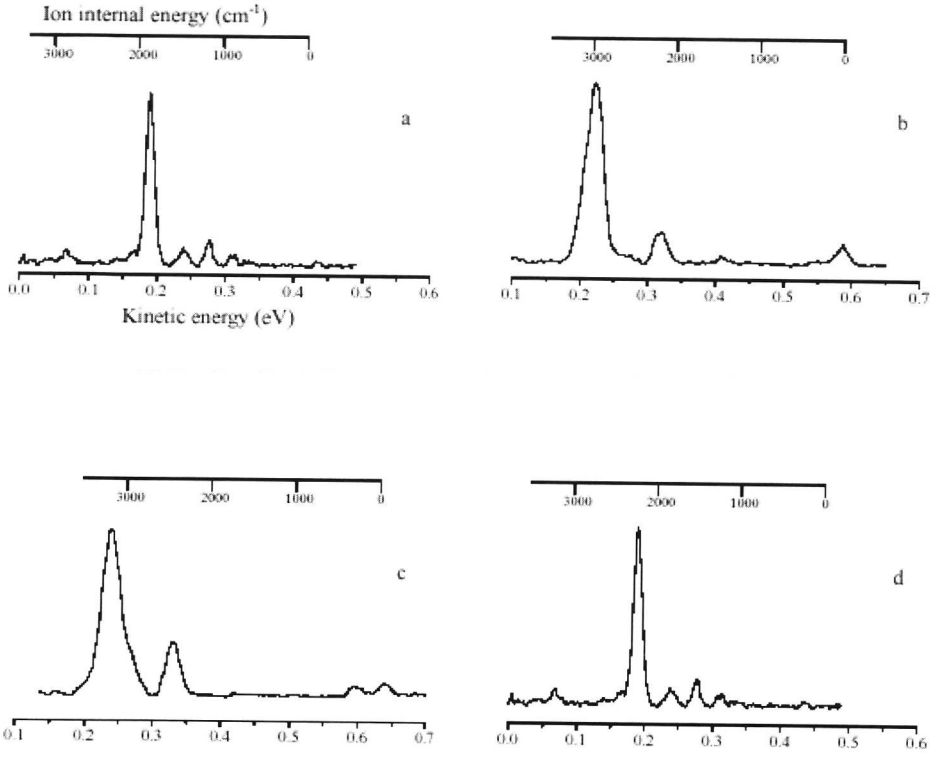

***Figure 3.6**: (3+1) Photoelectron spectra of acetone-d_6 at (a) 61327 cm^{-1} ($(3p_x)\,5_0^2$) and (d) 61597 cm^{-1} ($(3p_y)\,2_0^1$), and of acetone-h_6 at (b) 62241 cm^{-1} ($(3p_y)\,2_0^1$) and (c) 62559 cm^{-1} ($(3p_y)\,2_0^1 8_0^1$).*

For acetone-h_6 the $(3p_z)\,4_0^1$ transition was previously observed using two-photon excitation at 61467 cm^{-1}, but for acetone-d_6 this transition was not reported. In the present (3+1) experiments we indeed observe and confirm with photoelectron spectroscopy this transition at 61470 cm^{-1}, but moreover find that for acetone-d_6 the same transition occurs at 61105 cm^{-1}, *i.e.*, 1022 cm^{-1} shifted from the $3p_z$ origin. Ionisation *via* this resonance leads to a photoelectron spectrum with an intense peak

shifted by 127 meV (1024 cm^{-1}) from the 0"-0^+ peak, in agreement with a $\nu_4^+=1$ assignment. Furthermore, a peak shifted by 216 meV (1742 cm^{-1}) is present that exactly matches the energy where one would expect a signal associated with ionisation of a $3p_x$ vibrational level.

The peak in the excitation spectrum of acetone-d_6 at 61327 cm^{-1} has neither been reported before. Ionisation at this energy leads to the photoelectron spectrum displayed in Figure 6a that has an intense peak shifted by 243 meV (1960 cm^{-1}) from the 0"-0^+ peak. We assign this peak to the $\nu_5^+=2$ level because of the presence of a peak at 122 meV (984 cm^{-1}) that is assignable to $\nu_5^+=1$. On the basis of the excitation energy and this photoelectron spectrum, we conclude that the resonance should be assigned as the $(3p_x)5_0^2$ transition. Corroboration of this assignment is found in the presence of the $(3p_x)5_0^1$ transition in the (2+1) results. Peaks shifted by 154 and 194 meV in the photoelectron spectrum originate from coupling with the $3p_y$ and $3p_z$ states.

For acetone-h_6 vibronic transitions to CH stretch vibrational levels of the 3p Rydberg states would, energetically speaking, take place in the region around 62250 cm^{-1}. It is good to realise that *a priori* one would not expect to see vibronic transitions to these kind of levels since that would imply that the geometry of the molecule changes along these vibrational coordinates. Since it is a non-bonding lone-pair electron, mainly localised on the oxygen atom, that is excited, it would be hard to rationalise such geometry changes. Moreover, if such transitions were visible in the excitation spectra of the 3p Rydberg states, one may expect the same Franck-Condon factors for ionisation from the ground state, *i.e.*, such transitions should then also appear in He(I) photoelectron spectra. Since this is not the case [41], any vibronic activity in this energy region points to an unusual situation.

Our (3+1) excitation spectrum displays two intense peaks at 62241 and 62559 cm^{-1}. Xing *et al.* reported a similar pair of transitions, shifted, however, by 50 cm^{-1} to the red (62193 and 62517 cm^{-1}, respectively) [11]. Based on the spectra shown in Refs. [7] and [11], the energy difference between the two peaks, and the observed

difference between jet-cooled and room-temperature excitation spectra, we assume that we deal here with the same transitions, and that the shift is only due to different experimental conditions. These resonances were previously assigned as a "local origin" and as the "local origin + ν_8" [7]. They concluded that this local origin corresponds to a vibrational subband of the $3p_y$ transition that has been enhanced by the energetically proximal $^1A_1$ ($\pi\pi^*$) valence transition. In the original three-photon excitation work [11] the local origin was assigned as the $(3p_y)2_0^1$ transition, but this assignment was not repeated in the subsequent study [7]. The assignment to the $(3p_y)2_0^1$ transition implies that the frequency of the ν_2 vibration is reduced tremendously from 2937 cm^{-1} in the ground state to only 2425 cm^{-1} in the $3p_y$ state. This reduction was taken as evidence for a strong vibronic coupling between the $3p_y$ and the $\pi\pi^*$ excited states *via* ν_2, which - since the $3p_y$ is the lower of the two states - would lead to a decrease of the frequency of ν_2 in the $3p_y$ state and a (non-confirmed) increase in the $\pi\pi^*$ state.

The photoelectron spectrum obtained at 62241 cm^{-1} (Figure 6b) displays a small 0"-0^+ peak and an intense peak, shifted by 368 meV (2947 cm^{-1}). The location of this peak peak would be consistent with the formation of ionisation to the $\nu_2^+=1$ level (see Table I), and thus with an assignment of the resonance as $(3p_y)2_0^1$. There remains a catch, however, because the energy of 368 meV in the photoelectron spectrum matches also "exactly" the energy expected for ionisation of a $3p_x$ vibrational level. Alternatively, one might therefore assign the resonance to excitation and ionisation of a vibrational level of the $3p_x$ Rydberg state. The totally-symmetric nature of the transition [11] dictates, however, that the excited vibrational level is of A_2 symmetry. This implies (i) that the bright state in excitation is not that particular vibrational level of the $3p_x$ state, and (ii) that such a level has become accessible by vibronic coupling with the $3p_y$ state, which should thus be the bright state in excitation. One way to reconcile these observations is to say that it is indeed the $(3p_y)2_0^1$ transition that provides the transition moment for excitation, but because of the short-lived nature of

the $3p_y$ state - which will only be enhanced by the proximity of the $(3p_y)2^1$ level to the perturbing $\pi\pi^*$ state - the $3p_x$ state becomes the bright state in the ionisation process. The photoelectron spectrum shows two additional peaks. The small peak, shifted by 175 meV (1411 cm^{-1}) from the 0"-0^+ derives from ionisation to the $\nu_4^+=1$ level, while coupling with the $3p_z$ state leads to the signal at 256 meV (2065 cm^{-1}).

Table 3.5: *Observed three-photon transitions to higher-lying Rydberg states of acetone-h_6 and -d_6.*

acetone-h_6		acetone-d_6		
$\bar{\nu}$ (cm^{-1})	(n-δ)	$\bar{\nu}$ (cm^{-1})	(n-δ)	assignment
65250		65325	2.91	$3d_{x^2-y^2}$ ($^1B_2$) 0_0^0
65628		65604		$3d_{x^2-y^2}$ 8_0^1
65910	2.98	65865	2.97	$3d_{xy}$ ($^1B_1$) 0_0^0
		66159		$3d_{x^2-y^2}$ 6_0^1
		68961	3.43	$4p_x$ ($^1A_2$) 0_0^0
		69339	3.50	$4p_z$ ($^1B_2$) 0_0^0
		70041		$4p_x$ 4_0^1
71553	4.03	71511	4.02	4d 0_0^0
71890	4.14	71835	4.12	5s 0_0^0
73902	4.98	73844	4.96	5d 0_0^0
74170	5.15	74145	5.14	6s 0_0^0
75258	6.01	75208	5.97	6d 0_0^0
75420	6.17	75384	6.13	7s 0_0^0
76068	7.01	76017	6.93	7d 0_0^0
76176	7.19	76134	7.12	8s 0_0^0

The peak at 62559 cm^{-1} in our acetone-h_6 excitation spectrum, previously assigned as "local origin + ν_8" [7], does not resolve this ambiguity. The associated photoelectron spectrum (Figure 6c) displays a small peak shifted by 42 meV (341 cm^{-1}) from the 0"-0^+ peak, consistent with formation of $\nu_8^+=1$ ions. The most intense peak

is shifted by 400 meV (3230 cm^{-1}) and agrees both with ionisation to the $2^1 8^1$ ionic level and with ionisation of a $3p_x$ vibrational level.

More information is obtained from the acetone-d_6 spectra. Here, a relatively intense resonance is observed at 61597 cm^{-1} that is shifted by 2234 and 1762 cm^{-1} from the $3p_x$ and $3p_y$ origins, respectively. The strongest peak in the photoelectron spectrum (Figure 6d) is shifted by 280 meV (2258 cm^{-1}) from the 0"-0^+ peak. Table II indicates that this energy is at odds with a $\nu_2^+=1$ assignment, but agrees perfectly with the ionisation signal of a $3p_x$ vibrational level expected at 278 meV from the 0"-0^+ peak. This observation would thus favour the explanation based on the $(3p_y)2^1$ state being the bright state in excitation, and the coupled $3p_x$ state the bright state in ionisation. Figure 6d displays two additional small bands shifted by 231 and 191 meV. The latter band agrees with the expected position for ionisation of the $3p_z$ state (188 meV). The former band is assigned to ionisation of $3p_y$ vibrational levels that are populated by IVR. This would account for the observed difference between the 1762 cm^{-1} (218 meV) spacing in excitation and the 231 meV spacing in the photoelectron spectrum.

3.3.2.2. 65 000 – 71 000 cm^{-1} (8.0 – 8.8 eV) spectral region.

For excitation energies superseding the 3p Rydberg states the signals decrease dramatically in intensity, and it is not always possible to obtain excitation and photoelectron spectra under jet-cooled conditions with a sufficient signal-to-noise ratio to allow their detailed analysis. We have therefore recorded in most cases spectra under both jet-cooled as well as effusive conditions. As indicated already previously, three-photon excitation itself leads to rather broad resonances. The difference in resolution between jet-cooled and effusive conditions is therefore generally not dramatic. Resonances found in this energy region are tabulated in Table V.

This part of the spectrum is dominated by two peaks found at 65250 and 65910 cm^{-1} in acetone-h_6, and 65325 and 65865 cm^{-1} in -d_6. Previous (3+1) REMPI

experiments located the three-photon origin transitions to the $3d_{x^2-y^2}$ (3^1B_2) and $3d_{xy}$ (2^1B_1) Rydberg states at 65293 and 65944 cm^{-1} (65352 and 65987 cm^{-1} for -d_6) , respectively [7]. Compared to these numbers, we thus find here for acetone-h_6 red shifts of 43 and 34 cm^{-1}, respectively, that are probably caused by the different experimental conditions, and the fact that the resonances are rather broad. Indeed, photoelectron spectra recorded at these resonances confirm that they concern 0-0 transitions. As is by now expected, the photoelectron spectra also show that the states are extensively coupled to the lower-lying 3p Rydberg states. The vibrational development is rather restricted: for acetone-h_6 we find and confirm by photoelectron spectroscopy the previously proposed $(3d_{x^2-y^2})8_0^1$ transition at 65628 cm^{-1}, for acetone-d_6 the $(3d_{x^2-y^2})8_0^1$ transition at 65604 cm^{-1} and the $(3d_{x^2-y^2})6_0^1$ transition at 66159 cm^{-1}.

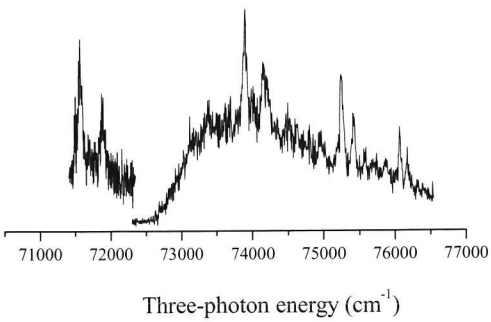

Figure 3.7: *(3+1) REMPI spectrum of room-temperature acetone-h_6 in the region of 71000 - 76500 cm^{-1}. The spectrum has been obtained employing two different dyes in the two indicated scans.*

The quantum defects of the 3p states lead us to expect transitions to the 4p states to occur around 69000 cm^{-1}. Indeed, for acetone-h_6 two origin transitions have previously been assigned at 68999 and 69348 cm^{-1}, respectively [7], while for acetone-d_6 these transitions were located at 68793 and 69350 cm^{-1}. In the present

study the transitions in this spectral region were so weak for acetone-h_6 that neither under jet-cooled, nor under effusive conditions a decent excitation spectrum could be obtained. For acetone-d_6, on the other hand, the (3+1) REMPI spectrum showed distinct peaks at 68961 and 69339 cm^{-1} for which photoelectron spectra indicated that they should be assigned as origin transitions. In passing by, we notice that also in the three-photon excitation study of Merchan *et al.* [7] the reported acetone-h_6 spectrum had a significant lower signal-to-noise ration in this region than the -d_6 spectrum. These transitions most logically would be assigned to the two 4p states assigned previously, were it not that the transition at 68961 cm^{-1} seems rather much displaced from the reported value of 68793 cm^{-1} [5]. *A posteriori* we notice, however, that the values of Merchan *et al.* imply a negative isotope shift of 206 cm^{-1} for the 68999 cm^{-1} transition, which is at odds with the values of isotope shifts of the other transitions observed so far: apart from a small negative value for the $3p_z$ excitation, only positive values were found. The transition energy of 68793 cm^{-1} is therefore most likely incorrectly reported.

Comparison with the splittings in the 3p manifold enables us to assign the two origin transitions. The energy difference between them is 378 cm^{-1} and is expected to be roughly proportional to $1/n^{*3}$. That means that an analogous energy difference of around 1000 cm^{-1} can be expected in the 3p manifold. The two Rydberg states having an energy difference that comes close to this value are the $3p_x$ and $3p_z$ Rydberg states. An additional argument for the implied non-observability of the $4p_y$ Rydberg state is that we can expect this state to be short-lived on account of its coupling with the $\pi\pi^*$ state. These arguments strongly favour an assignment of the peaks at 68961 and 69339 cm^{-1} to the $4p_x$ and $4p_z$ Rydberg states, respectively.

3.3.2.3. 71 000 – 76 500 cm^{-1} (8.8 – 9.5 eV) spectral region.

The jet-cooled (3+1) REMPI spectrum of acetone-h_6 in the spectral region of 71000–76500 cm^{-1} is shown in Figure 7. In order to have sufficient signal intensity,

the spectrum was recorded in the two indicated scans using Exalite 416 and 404 for the 71500-72500 and 72500-76500 cm^{-1} regions, respectively. Efforts to record spectra between 72000 and 73500 cm^{-1} with Exalite 411 were not successful due to low dye gain. An analogous spectrum (not shown) was obtained for acetone-d_6. Effusive (3+1) REMPI spectra show similar results, albeit that the maxima of the peaks are shifted by 30-40 cm^{-1} to the red. The spectra show eight resonances whose positions are given in Table V. The resonances observed in the present study match well peaks observed in previous one-photon work [31], although in that work an assignment was not attempted.

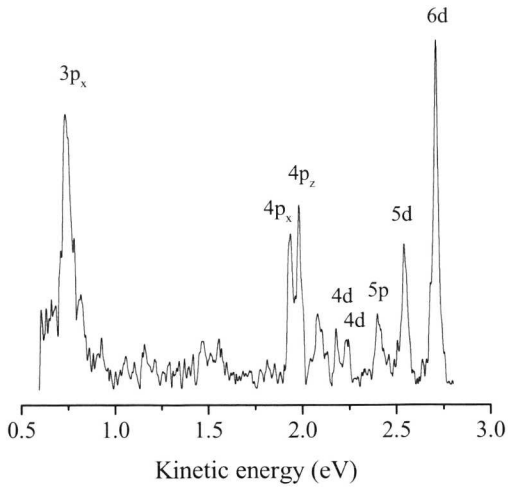

***Figure 3.8**: (3+1) Photoelectron spectrum of acetone-h_6 via the 0-0 transition to the 6d Rydberg state at 75258 cm^{-1}.*

Because of the low signal intensities, photoelectron spectra have been recorded under effusive conditions. These spectra demonstrate that the resonances are associated with origin transitions. In general, the photoelectron spectra show that the states excited at these energies are subject to extensive coupling with lower lying

Rydberg states. An example is shown in Figure 8 where ionisation occurs *via* the resonance assigned to the 6d manifold. Apart from ionisation to the vibrationless level of the ion, extensive ionisation occurs to high vibrational ionic levels. Under the assumption of a $\Delta v=0$ ionisation behaviour, we can calculate what excitation energy is associated with each peak in the photoelectron spectrum. As indicated in Figure 8, these excitation energies agree well with the excitation energies of Rydberg states determined previously and in the present study. Apart from states that were already known, the photoelectron spectra also enable us to observe and assign states that we have not observed as resonances in the excitation spectra - in this particular case, for example, the 5p Rydberg states.

Calculation of the quantum defect associated with each of the observed transitions in the excitation spectrum leads to the conclusion that members are observed of two Rydberg series with quantum defects of approximately 0 and 0.85. The first series can be grouped nicely with the $^1B_1(n\rightarrow 3d_{xy})$ transition observed at 65910 cm^{-1}, and allows us to conclude that this concerns an nd Rydberg series of which we have now identified the n=3-7 members. The second series is assigned to the ns series, of which the first member is the in the introduction mentioned 3s state located at 51232 cm^{-1}. The states excited in the present experiments are described by the excitation of an electron from the nonbonding lone pair orbital that in first approximation can be represented by the $2p_y$ orbital on the oxygen atom. Atomic selection rules then dictate a $\Delta l=\pm 1$ propensity for one-photon excitation, and a $\Delta l=\pm 1,\pm 3$ propensity for three-photon excitation. The present assignment to ns and nd Rydberg states is thus in good agreement with such expectations.

3.4 CONCLUSIONS.

The application of photoelectron spectroscopy to characterise excited states of acetone-h_6 and -d_6 has led to a detailed picture of the spectroscopic properties of excited states of acetone, and of some vibrational properties of the ground state of the

radical cation. In particular for the 3p Rydberg states, the present study has modified and extended assignments proposed in previous multiphoton ionisation studies. Apart from the characterization of previously observed states, some eight new Rydberg states have been identified and studied. The observed photoelectron spectra give in all cases evidence for an important role of vibronic coupling in determining the observable spectroscopic properties of the excited states under investigation. This has been exemplified to the extreme for 3p Rydberg states where the state that is excited in the multiphoton excitation process could be projected on the basis of the $3p_x$, $3p_y$, and $3p_z$ states. One of the dominating coupling pathways, which is not directly visible in the photoelectrons spectra, but can be deduced from the combination of excitation and ionziation properties of excited states, is that between the $\pi\pi^*$ ($^1A_1$) excited valence state and Rydberg states of A_1 symmetry. Because of the short-lived nature of the former state, Rydberg states of A_1 symmetry lose intensity in excitation and ionisation, but ultimately reveal themselves once again by vibronic coupling with longer-lived Rydberg states. Although vibronic coupling of the $\pi\pi^*$ excited valence state with Rydberg states of other symmetries is theoretically possible, it has been shown that for these states other vibronic couplings prevail. These pathways do become nicely visible in the photoelectron spectra and concern the intra-, *e.g.*, between the 3p components, and interstate, *e.g.*, between 7d and 3p, couplings between all other Rydberg states. Because of this coupling, excitation energies of states that were not visible in our excitation spectra, *e.g.*, the 4p and 5p Rydberg states, could be determined from photoelectron spectra taken at higher excitation energies.

REFERENCES.

[1] M. Merchan and B.O. Roos, Theor. Chim. Acta **92**, 227 (1995).

[2] P.J. Bruna, M.R.J. Hachey, and F. Grein, Mol. Phys. **94**, 917 (1998).

[3] A.B. Rocha and C.E. Bielschowsky, Chem. Phys. **253**, 51 (2000).

[4] B. Hess, P.J. Bruna, R.J. Buenker, and S.D. Peyerimhoff, Chem. Phys. **18**, 267 (1976).

[5] V. Galasso, J. Chem. Phys. **92**, 2495 (1990).

[6] S.R. Gwaltney and R.J. Bartlett, Chem. Phys. Letters **241**, 26 (1995).

[7] M. Merchan, B.O. Roos, R. McDiarmid, and X. Xing, J. Chem. Phys. **104**, 1791 (1996).

[8] D.W. Liao, A.M. Mebel, M. Hayashi, Y.J. Shiu, Y.T. Chen and S.H. Lin, J. Chem. Phys. **111**, 205 (1999).

[9] Shimanouchi, Tables of molecular vibrational frequencies. Consolidated Vol. I, Natl. Stand. Ref. Data Ser., Natl, Bur. Stand. Circ. No. 39. (U.S. GPO, Washington, D.C., 1972), pp 123-125

[10] D.A. Shea, L. Goodman, and M.G. White, J. Chem. Phys. **112**, 2762 (2000).

[11] X. Xing, R. McDiarmid, J.G. Philis, and L. Goodman, J. Chem. Phys. **99**, 7565 (1993).

[12] J.G. Philis, J.M. Berman, and L. Goodman, Chem. Phys. Letters **167**, 16 (1990).

[13] T. Kundu, S.N. Thakur, and L. Goodman, J. Chem. Phys. **97**, 5410 (1992).

[14] J.G. Philis and L. Goodman, J. Chem. Phys. **98**, 3795 (1993).

[15] R.T. Wiedmann, L. Goodman, and M.G. White, Chem. Phys. Letters **293**, 391 (1998).

[16] H. Zuckermann, Y. Haas, M. Drabbels, J. Heinze, W.L. Meerts, J. Reuss, and J. van Bladel, Chem. Phys. **163**, 193 (1992).

[17] E.E. Barnes and W.T. Simpson, J. Chem. Phys. **39**, 670 (1963).

[18] R.H. Huebner, R.J. Celotta, S.R. Mielczarek, and C.E. Kuyatt, J. Chem. Phys. **59**, 5434 (1973).

[19] W.M. St. John III, R.C. Estler, and J.P. Doering, J. Chem. Phys. **61**, 763 (1974).

[20] K.N. Walzl, C.F. Koerting, and A. Kupperman, J. Chem. Phys. **87**, 3796 (1987).

[21] D.J. Donaldson, G.A. Gaines, and V. Vaida, J. Phys. Chem. **92**, 2766 (1988).

[22] M. Baba, I. Hanazaki, and U. Nagashima, J. Chem. Phys. **82**, 3938 (1985).

[23] G.A. Gaines, D.J. Donaldson, S.J. Strickler, and V. Vaida, J. Phys. Chem. **92**, 2762 (1988).

[24] A. Gedanken and R. McDiarmid, J. Chem. Phys. **92**, 3237 (1990).

[25] R. McDiarmid, J. Chem. Phys. **95**, 1530 (1991).

[26] P. Brint, L. O'Toole, S. Couris, and D. Jardine, J. Chem. Soc. Faraday Trans. **87**, 2891 (1991).

[27] R. McDiarmid and A. Sabljic, J. Chem. Phys. **89**, 6086 (1988).

[28] S.N. Thakur, D. Guo, T. Kundu, and L. Goodman, Chem. Phys. Letters **199**, 335 (1992).

[29] R. McDiarmid and X. Xing, J. Chem. Phys. **107**, 675 (1997)

[30] W.A. Noyes, A.B.F. Duncan, and W.M. Manning, J. Chem. Phys. **2**, 717 (1934).

[31] A.B.F. Duncan, J. Chem. Phys. **3**, 131 (1935).

[32] R.A. Morgan, P. Puyuelo, J.D. Howe, M.N.R. Ashfold, W.J. Buma, J.B. Milan, and C.A. de Lange, J. Chem. Soc. Faraday Trans. **90**, 3591 (1994).

[33] R.A. Morgan, P. Puyuelo, J.D. Howe, M.N.R. Ashfold, W.J. Buma, N.P.L.Wales, and C.A. de Lange, J. Chem. Soc. Faraday Trans. **91**, 2715 (1995)

[34] R.A. Morgan, A.J. Orr-Ewing, M. N.R. Ashfold, W.J. Buma, N.P.L. Wales, and C.A. de Lange, J. Chem. Soc. Faraday Trans. **91**, 3339 (1995).

[35] V. Blanchet, M.Z. Zgierski, and A. Stolow, J. Chem. Phys. **114**, 1194 (2001).

[36] M. Schmitt, S. Lochbrunner, J.P. Shaffer, J.J. Larsen, M.Z. Zgierski, and A. Stolow, J. Chem. Phys. **114**, 1206 (2001)

[37] C.R. Scheper, W.J. Buma, and C.A. de Lange, J. Electron Spectrosc. Relat. Phenom. **109**, 8319 (1998).

[38] A.M. Rijs, E.H.G. Backus, C.A. de Lange, N.P.C. Westwood, and M.H.M. Janssen, J. Electron Spectrosc. Relat. Phenom. **112**, 151 (2000).

[39] P. Kruit and F.H. Read, J. Phys. E. **16**, 313 (1983).

[40] C.E. Moore, Atomic Energy Levels, Natl. Bur. Stand. (U.S.) circ. No. 35 (U.S. GPO. Washington D.C., 1971) Vol. II.

[41] K. Furuya, S. Katsumata, and K. Kimura, J. Electron Spectrosc. Relat. Phenom. **62**, 237 (1993).

[42] M.J. Frisch, J.A. Pople, and J.S. Binkley, J. Chem. Phys. **80**, 3265(1984).

[43] J.B.Foresman, M. Head-Gordon, J.A.Pople, and M.J. Frisch, J. Chem.Phys. **96**, 135 (1992).

[44] Becke, A.M., J. Chem. Phys. **98**, 5648 (1993).

[45] M.J. Frisch, G.W. Trucks, H.B. Schlegel, G.E. Scuseria, M.A. Robb, J.R. Cheeseman, V.G. Zakrzewski, J. Montgomery, R.E. Stratmann, J.C. Burant, S. Dapprich, J.M. Millam, A.D. Daniels, K.N. Kudin, M.C. Strain, O. Farkas, J. Tomasi, V. Barone, M. Cossi, R. Cammi, B. Mennucci, C. Pomelli, C. Adamo, S. Clifford, J. Ochterski, G.A. Petersson, P.Y. Ayala, Q. Cui, K. Morokuma, D.K. Malick, A.D. Rabuck, K. Raghavachari, J.B. Foresman, J. Cioslowski, J.V. Ortiz, B.B. Stefanov, G. Liu, A. Liashenko, P. Piskorz, I. Komaromi, R. Gomperts, R.L. Martin, D.J. Fox, T. Keith, M.A. Al-Laham, C.Y. Peng, A. Nanayakkara, C. Gonzalez, M. Challacombe, P.M.W. Gill, B. Johnson, W. Chen, M.W. Wong, J.L. Andres, C. Gonzalez, M. Head-Gordon, E.S. Replogle, J.A. Pople, Gaussian 98, Revision A.5; Gaussian, Inc.: Pittsburgh PA, 1998.

[46] (a) M. Born and J.R. Oppenheimer, Ann. Phys., **84**, 457 (1927); (b) M. Born, Nachr. Akad. Wiss. Gottingen, Math.-Phys. **KL**, IIa, P1 (1951); (c) M. Born and K. Huang, *Dynamics of Crystal Lattice* (Oxford University, New York, 1954).

[47] W.M. McClain and R.A. Harris, in *Excited States*, edited by E.C. Lim (Academic, New York, 1977), Vol. 3, pp. 1-56.

[48] A.P. Scott and L. Radom, J. Phys. Chem. **100**, 16502 (1996).

[49] W.C. Harris and I.W. Levin, J. Mol. Spectrosc. **43**, 117 (1972).